

Atomic disorder effects on half-metallicity of the full-Heusler alloys $\text{Co}_2(\text{Cr}_{1-x}\text{Fe}_x)\text{Al}$: A first-principles study

Yoshio Miura, Kazutaka Nagao, and Masafumi Shirai

Research Institute of Electrical Communication, Tohoku University, Katahira 2-1-1, Aoba-ku, Sendai 980-8577, Japan

(Received 20 September 2003; revised manuscript received 29 December 2003; published 12 April 2004)

We investigate the atomic disorder effects on the half-metallicity of the full-Heusler alloy $\text{Co}_2(\text{Cr}_{1-x}\text{Fe}_x)\text{Al}$ from first principles by using the Korringa-Kohn-Rostoker method with the coherent potential approximation. Our results show that disorder between Cr and Al does not significantly reduce the spin polarization of the parent alloy Co_2CrAl , while disorder between Co and Cr makes a considerable reduction of the spin polarization. It is observed that the spin polarization of $\text{Co}_2(\text{Cr}_{1-x}\text{Fe}_x)\text{Al}$ decreases with increasing Fe concentration x in both the ordered $L2_1$ and the disordered $B2$ structures, and that the effects of the disorder on the spin polarization is significant at low Fe concentrations. The results suggest that a highly spin-polarized ferromagnet with high Curie temperature will be obtained if a $\text{Co}_2(\text{Cr}_{1-x}\text{Fe}_x)\text{Al}$ with the ordered $L2_1$ structure can be fabricated at low Fe concentrations.

DOI: 10.1103/PhysRevB.69.144413

PACS number(s): 75.50.Cc, 71.20.Be, 71.20.Lp, 71.23.-k

I. INTRODUCTION

Challenge to utilizing spin degree of freedom of electrons as well as their charge in electronic applications (spintronics) has drawn much attention in recent years.¹⁻³ A prototype material of this concept is half-metallic ferromagnet (HMF), in which majority-spin band is metallic, while minority-spin band is semiconducting with an energy gap at the Fermi level, leading to complete (= 100%) spin polarization. The HMF acts as a spin filter which provides current with a high degree of spin polarization. This feature is of great importance in spin-dependent devices, such as tunneling magnetoresistance (TMR) device,⁴ which is essential for creation of ultrahigh density magnetic random access memory. The HMF was first proposed by de Groot *et al.*⁵ from the band-structure calculations for the $C1_b$ -type Heusler alloys (half-Heusler), NiMnSb and PtMnSb. So far, various kinds of the HMF's have been studied, such as the rutile-type CrO_2 ,⁶ the transition-metal perovskites $\text{La}_{0.7}\text{Sr}_{0.3}\text{MnO}_3$,⁷ $L2_1$ -type Heusler alloys (full-Heusler),⁸⁻¹³ other half-Heusler alloys,¹⁴ zinc-blende type MnAs, CrAs, and CrSb.¹⁵⁻¹⁷

Although many compounds have been predicted to be HMF, there are tremendous difficulties in experimentally demonstrating the half-metallicity of these compounds due to the sensitivity of spin polarization to structural disorder, surface/interface stoichiometry, etc.¹⁸⁻²⁴ Caballero *et al.*²⁰ performed measurements of current-perpendicular-to-plane magnetoresistance (CPP-MR) of NiMnSb/Cu/NiMnSb spin-valve structures at 4.2 K, and obtained the CPP-MR of 5–10 %, which is much smaller than the complete spin-valve effect expected from the HMF. They attributed the small CPP-MR to the disordered NiMnSb and NiMnSb/Cu interfaces. Geiersbach *et al.*²⁴ grew (110) thin films of Co_2MnSi , Co_2MnGe , and Co_2MnSn on top of a $\text{MgO}(001)$ substrate, and reported that the electrical conductivity is rather low indicating structural disorder.

Block *et al.*^{12,13,25} have found that pressed powder compacts of the full Heusler alloy $\text{Co}_2(\text{Cr}_{0.6}\text{Fe}_{0.4})\text{Al}$ have the

disordered $B2$ structure and show a large magnetoresistive effect of 30% in a small magnetic field at room temperature (RT). Furthermore, Inomata *et al.*²⁶ have shown that a magnetic tunneling junction based on a Heusler alloy $\text{Co}_2(\text{Cr}_{0.6}\text{Fe}_{0.4})\text{Al}$ with the disordered $B2$ structure consisting of $\text{Co}_2(\text{Cr}_{0.6}\text{Fe}_{0.4})\text{Al}/\text{AlO}_x/\text{CoFe}/\text{NiFe}/\text{IrMn}/\text{Ta}$ has a relatively large TMR of 16% at RT (26.5% at 5 K). These experimental results suggest that the atomic disorder among Cr, Fe, and Al in $\text{Co}_2(\text{Cr}_{0.6}\text{Fe}_{0.4})\text{Al}$ does not significantly reduce the spin polarization, while it was considered that the atomic disorder destroys their high spin polarization for the half-metallic Heusler alloy NiMnSb.^{27,28}

The electronic and magnetic properties of $\text{Co}_2(\text{Cr}_{1-x}\text{Fe}_x)\text{Al}$ with the ordered $L2_1$ structure have been investigated using the first-principles calculation.^{11-13,29} It was found that the ordered $\text{Co}_2(\text{Cr}_{1-x}\text{Fe}_x)\text{Al}$ has a high spin polarization, and its total magnetic moment follows the Slater-Pauling behavior $M_t = Z_t - 24$, where M_t is the total magnetic moment in μ_B per unit cell and Z_t is the total number of valence electrons, which scales linearly with the Fe concentration x . It was also found that Co_2CrAl with ordered $L2_1$ structure retain a high spin polarization at the CrAl-terminated (001) surfaces.³⁰ These calculation results suggest that $\text{Co}_2(\text{Cr}_{1-x}\text{Fe}_x)\text{Al}$ with the ordered $L2_1$ structure is promising material for spintronics devices. However, it is not clear that $\text{Co}_2(\text{Cr}_{1-x}\text{Fe}_x)\text{Al}$ with the disordered structure has a high spin polarization.

In the present study, we focus our attention on the effects of atomic disorder on the half-metallicity of the full-Heusler alloy $\text{Co}_2(\text{Cr}_{1-x}\text{Fe}_x)\text{Al}$, using first-principles calculations. First, we investigate the effects of atomic disorder on the electronic and magnetic properties of the parent alloy Co_2CrAl . Then, we investigate the effects of substitution of Fe for Cr and discuss how the half-metallicity of the alloy changes by the Fe substitution and the atomic disorder among Cr, Fe, and Al.

II. METHODS

The calculations are performed using the *ab initio* calculation code based on the Korringa-Kohn-Rostoker method³¹

developed by Akai *et al.*³² and the atomic disorder calculations are implemented within the coherent potential approximation. The space is divided into nonoverlapping muffin-tin spheres. Our results are obtained by the so-called scalar-relativistic calculation, in which the spin-orbit interaction is neglected. We describe the spin degree of freedom within the collinear configuration. We adopt the generalized gradient approximation (GGA) (Ref. 33) for the exchange and correlation term, because the lattice constant and the magnetic moment of Co_2FeAl calculated on the basis of the GGA show good agreement with the experimental results^{34–36} in comparison with those of the local-density approximation.³⁷ The unit cell of the full-Heusler alloy Co_2CrAl with the $L2_1$ structure is a fcc lattice with four atoms as basis at $\text{Co}=(0,0,0)$ and $(\frac{1}{2}, \frac{1}{2}, \frac{1}{2})$ (octahedral site), $\text{Cr}=(\frac{1}{4}, \frac{1}{4}, \frac{1}{4})$, $\text{Al}=(\frac{3}{4}, \frac{3}{4}, \frac{3}{4})$ (tetrahedral site) in Wyckoff coordinates. We consider two types of disorder of the full-Heusler alloy, one is a Co-Cr type disorder corresponding to $(\text{Co}_{1-y/2}\text{Cr}_{y/2})_2(\text{Cr}_{1-y}\text{Co}_y)\text{Al}$, and the other is a Cr-Al type disorder corresponding to $\text{Co}_2(\text{Cr}_{1-y}\text{Al}_y)(\text{Al}_{1-y}\text{Cr}_y)$. For the Brillouin zone (BZ) integration, we have included 256 \mathbf{k} points in the full BZ.

III. RESULTS AND DISCUSSIONS

A. Atomic disorder effects

First, we have studied the effects of atomic disorder on the half-metallicity of the parent alloy Co_2CrAl . In Fig. 1, we show the spin polarization, the total energy relative to the ordered Co_2CrAl , and the total magnetic moment per unit cell in μ_B as a function of the disorder level y for the Co-Cr type disorder and the Cr-Al type disorder. The spin polarization P is defined by

$$P = \frac{D_{\uparrow} - D_{\downarrow}}{D_{\uparrow} + D_{\downarrow}}, \quad (1)$$

where D_{σ} denotes the majority (\uparrow) and minority (\downarrow) spin components in the density of states at the Fermi level. It is found that the Cr-Al type disorder does not significantly degrade the half-metallicity of Co_2CrAl , i.e., the spin polarization of Co_2CrAl is 0.97 in the ordered structure ($y=0.0$), and 0.93 in the disordered structure ($y=0.5$). On the other hand, the spin polarization linearly decreases with increasing the disorder level y in the Co-Cr type disorder. In this case, even the disorder level y of 0.1 makes a considerable reduction (more than 0.30) in the spin polarization. However, as shown in Fig. 1(b), the total energy of the Co-Cr type disorder relative to the ordered Co_2CrAl rapidly increases with increasing y compared with the Cr-Al type disorder. Thus, it is expected that the Co-Cr type disorder which degrades the half-metallicity of Co_2CrAl is unlikely to occur compared with the Cr-Al type disorder which does not significantly degrade the half-metallicity of the alloy. This means that the half-metallicity of Co_2CrAl is hardly influenced by the atomic disorder, and accordingly that the alloy is a good candidate for applications.

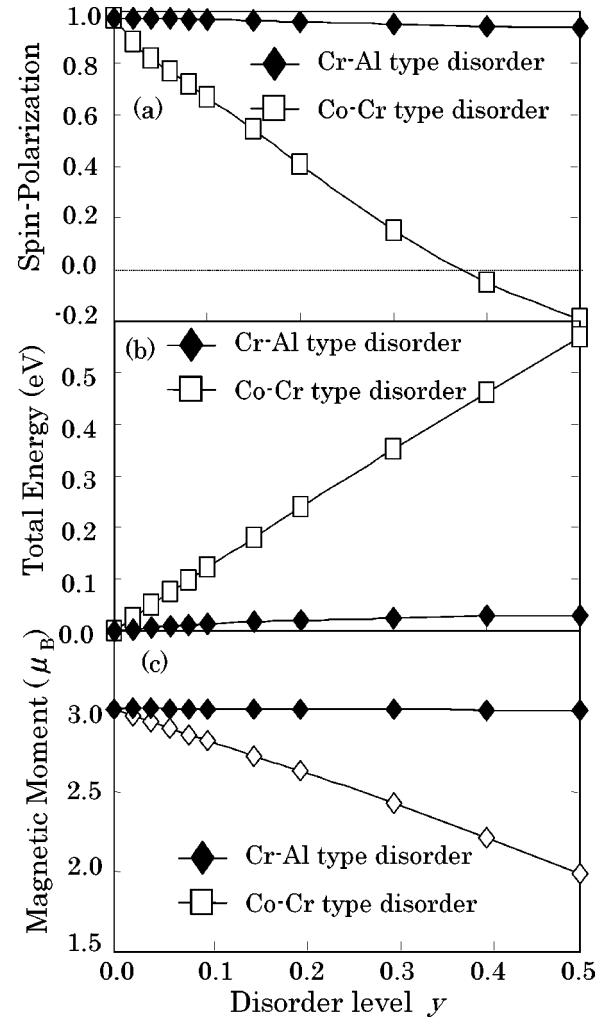


FIG. 1. (a) Spin polarization [see Eq. (1)], (b) total energy per unit cell relative to that of the ordered structure, and (c) total magnetic moment per unit cell of Co_2CrAl as a function of the disorder level y (see text).

To discuss why the Cr-Al type disorder does not significantly degrade the half-metallicity of Co_2CrAl , we present in Fig. 2 the density of states (DOS) and the atom orbital projected local density of states (LDOS) of Co_2CrAl with the ordered $L2_1$ structure and with the disordered $B2$ structure which corresponds to the Cr-Al type disordered structure with the disorder level of $y=0.5$. As shown in Fig. 2(a), Co_2CrAl has the half-metallic DOS in the disordered $B2$ structure as well as in the ordered $L2_1$ structure. This can be attributed to the orbital characters in the minority DOS near the Fermi level. By comparing the total DOS and the LDOS of Co $3d$, we found that the energy gap of the minority DOS near the Fermi level is mainly constructed of the Co $3d$ states. It is considered that a hybridization occurs not only between the first nearest neighbor Co $3d$ and Cr $3d$ orbital but also between the second nearest neighbor Co $3d$ and Co $3d$ orbital. The second nearest neighbor Co-Co interaction causes the nonbonding states in the minority DOS near the Fermi level,¹¹ and these states are localized at the Co site, and do not couple to the Cr $3d$ orbital. Thus, the disorder

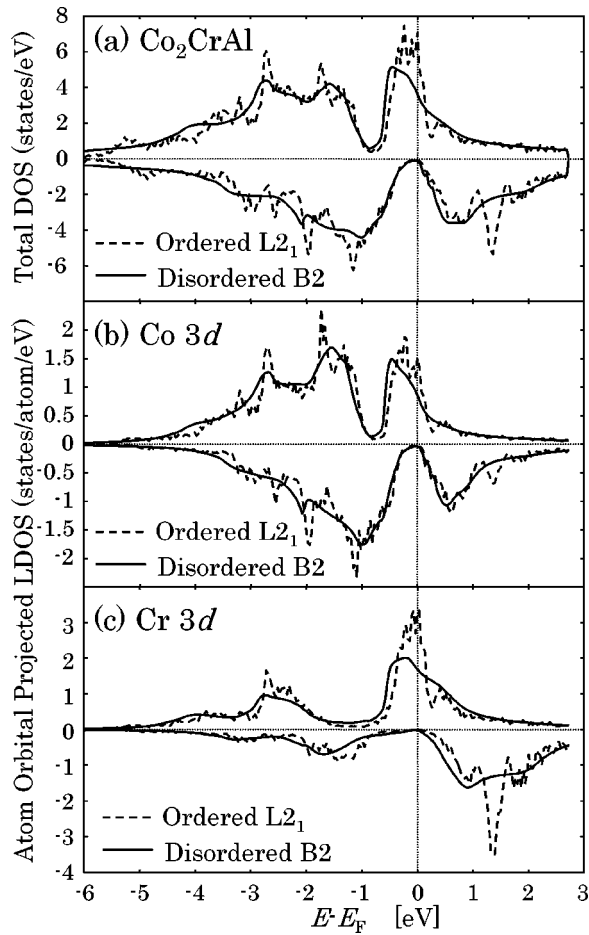


FIG. 2. Density of states of the majority-spin (positive) and the minority-spin (negative) components of Co_2CrAl with the ordered $L2_1$ structure (solid line) and with the disordered $B2$ structure (broken line). (a) Total DOS of Co_2CrAl . (b) Atom orbital projected local DOS for Co. (c) Atom orbital projected local DOS for Cr. The vertical dotted lines indicate the position of the Fermi level (E_F).

between Cr and Al does not significantly affect the electronic structure near the Fermi level, and therefore the semiconducting character of minority bands, is still kept even in the disordered $B2$ structure. The slight decrease of the spin polarization in the disordered $B2$ structure is due to the decrease of the majority DOS at the Fermi level. In Figs. 2(b) and 2(c), it is found that the peak of the majority DOS at the Fermi level in the ordered $L2_1$ structure is constructed of the Cr $3d$ orbital which hybridizes with the Co $3d$ orbital. Since the disorder between Cr and Al weakens the hybridization, the peak in the disordered $B2$ structure decreases as compared with the peak in the ordered $L2_1$ structure. These results are a contrast to the case of the half-Heusler alloy like NiMnSb. Orgassa *et al.*^{27,28} reported that the disorder between the Mn and Sb sites degrades the half-metallicity in NiMnSb. In this case, the disorder between Mn and Sb significantly influences the hybridization between Ni $3d$ and Mn $3d$ orbitals, and makes additional states in the energy gap of the minority DOS at the Fermi level.

Then, we discuss why the Co-Cr type disorder degraded the half-metallicity of Co_2CrAl . We show in Fig. 3 the DOS

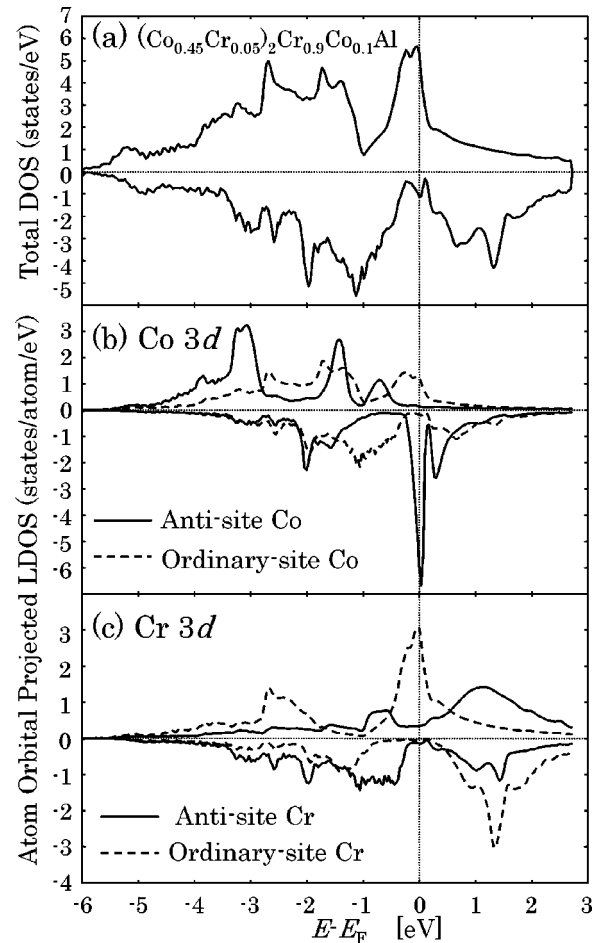


FIG. 3. Density of states of Co_2CrAl with the Co-Cr type disorder (the disorder level of 0.1). (a) Total DOS. (b) Atom orbital projected local DOS for Co. (c) Atom orbital projected local DOS for Cr.

and the LDOS of Co_2CrAl with the Co-Cr type disorder with $y=0.1$. One can find additional states in the minority DOS at the Fermi level. Figure 3(b) shows that the antisite Co $3d$ states mainly contribute to these additional states. From detailed analysis, we found that the additional minority DOS of the Co $3d$ at the Fermi level has $d_{3z^2-r^2}$ or $d_{x^2-y^2}$ orbital character. The energy levels of the antisite Co $3d_{3z^2-r^2}$ and $3d_{x^2-y^2}$ orbitals are located in the energy gap of the minority DOS. Thus, the spin polarization of Co_2CrAl is considerably reduced by the Co-Cr type disorder. Furthermore, as shown in Fig. 1(c), the total magnetic moment of Co_2CrAl decreases with increasing y in the Co-Cr type disorder and is lowered to $\approx 2.0\mu_B$ at $y=0.5$. This is due to the antiferromagnetic coupling of the antisite Cr with the first nearest-neighbor ordinary-site Cr. Contrary to this, in the Cr-Al type disorder, the magnetic moment is kept at $3.01\mu_B$ throughout the entire range of y in accordance with the Slater-Pauling behavior.¹¹⁻¹³

B. Fe substitutional effects

To investigate the effects of substitution of Fe for Cr on the half-metallicity of the parent alloy Co_2CrAl , we have

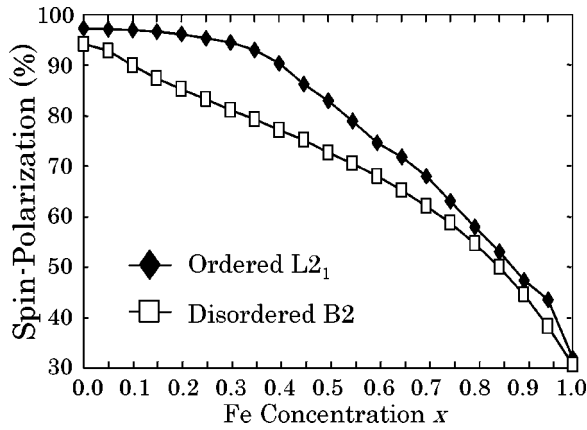


FIG. 4. Spin polarization as a function of the Fe concentration x in $\text{Co}_2(\text{Cr}_{1-x}\text{Fe}_x)\text{Al}$ with the ordered $L2_1$ structure (diamond) and the disordered $B2$ structure (square).

calculated the spin polarization of $\text{Co}_2(\text{Cr}_{1-x}\text{Fe}_x)\text{Al}$ with the ordered $L2_1$ structure and with the disordered $B2$ structure as a function of the Fe concentration x . It is found in Fig. 4 that the spin polarization decreases with increasing x both in the ordered $L2_1$ and the disordered $B2$ structures. The spin polarization remains high (more than 0.90) up to $x=0.35$, then decreases with increasing x in the ordered $L2_1$ structure, while it strongly decreases with increasing x in the disordered $B2$ structure. This leads to relatively large difference of the spin polarization between the ordered $L2_1$ and the disordered $B2$ structures at low Fe concentrations ($0.1 \leq x \leq 0.5$), although the difference is not so large (less than about 0.05) in the limiting cases of $x=0.0$ (Co_2CrAl) and $x=1.0$ (Co_2FeAl).

Figure 5 exhibits the DOS and the atom orbital projected LDOS for Co and Fe $3d$ of Co_2FeAl with the ordered $L2_1$ structure and the disordered $B2$ structure, which clearly show the effect of Fe substitution on the spin polarization. It is found from Fig. 5(a) that there is no peak in the majority DOS at the Fermi level, both in the ordered $L2_1$ and the disordered $B2$ structures. The peak at the Fermi level observed in the DOS of Co_2CrAl [see Fig. 2(a)] moves to an energy region far below the Fermi level to account for the two extra valence electrons of Co_2FeAl . This considerably reduces the spin polarization of Co_2FeAl . Furthermore, a few additional states are found in the minority DOS at the Fermi level. As is pointed out by Galanakis,²⁹ due to the strong hybridization between the Fe $3d$ and Co $3d$, it is energetically more favorable that the local magnetic moment of Co in Co_2FeAl is increased as compared with that of Co in Co_2CrAl . This leads to charge transfer from the Co minority-spin states to the Fe minority-spin states, and accordingly the Fe $3d$ minority conduction bands are shifted toward the Fermi level. This gives rise to additional states at the Fermi level [see Fig. 5(c)], and Co_2FeAl loses half-metallicity.

Next we look at the effects of the disorder in detail, especially at low Fe concentrations. The rapid decrease of the spin polarization with increasing x in the disordered $B2$ structure is mainly due to appearance of the Fe $3d$ minority

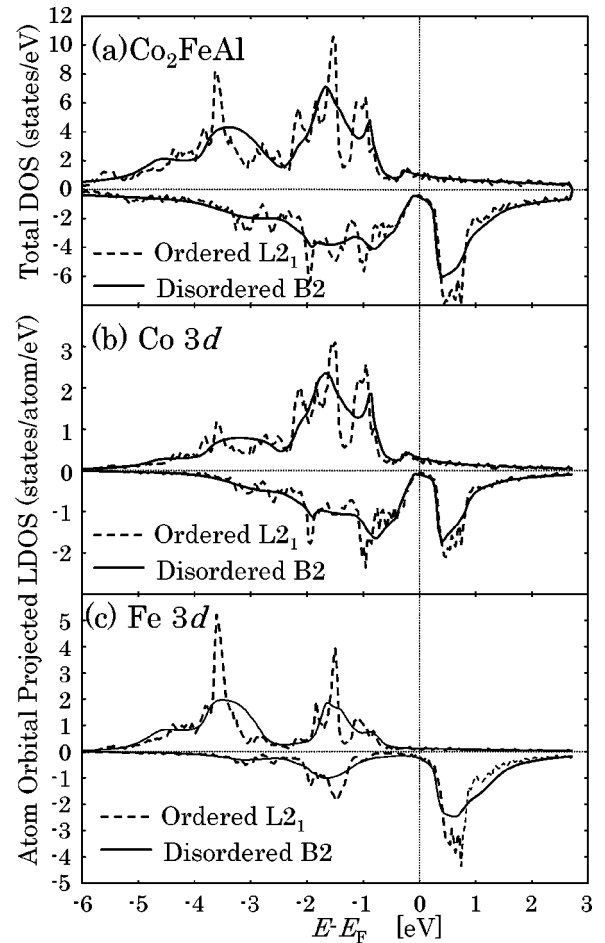


FIG. 5. Density of states of Co_2FeAl with the ordered $L2_1$ structure (solid line) and with the disordered $B2$ structure (broken line). (a) Total DOS. (b) Atom orbital projected local DOS for Co. (c) Atom orbital projected local DOS for Fe.

DOS at the Fermi level. We show in Fig. 6 the atom orbital projected LDOS of Fe $3d$ in $\text{Co}_2(\text{Cr}_{1-x}\text{Fe}_x)\text{Al}$ with the ordered $L2_1$ and the disordered $B2$ structures for (a) $x=0.1$, (b) $x=0.4$, and (c) $x=0.8$. It is found in Fig. 6(a) that at $x=0.1$, the Fermi level of the disordered $B2$ structure is at the left edge of the Fe minority conduction bands, while the Fermi level of the ordered $L2_1$ structure is in the energy gap of the minority DOS. It is considered that due to the lifetime effect caused by the atomic disorder, the Fe minority conduction bands of the disordered $B2$ structure are broadened much more than those of the ordered $L2_1$ structure. Thus, the additional states appear in the minority DOS at the Fermi level in the disordered $B2$ structure. This effect is, however, not clearly observed at larger x ($x=0.4$ and 0.8) because the Fe minority conduction bands are also broadened with increasing x even in the ordered $L2_1$ structure due to the strong hybridization between the Co $3d$ and Fe $3d$. We conclude that the atomic disorder scarcely influences the spin polarization at high Fe concentrations, and only at low Fe concentrations (except for $x=0.0$), it reduces the spin polarization of $\text{Co}_2(\text{Cr}_{1-x}\text{Fe}_x)\text{Al}$ with the disordered $B2$ structure.

Figure 7 shows the magnetic energy gain (the total energy difference between the ferromagnetic state and nonmagnetic

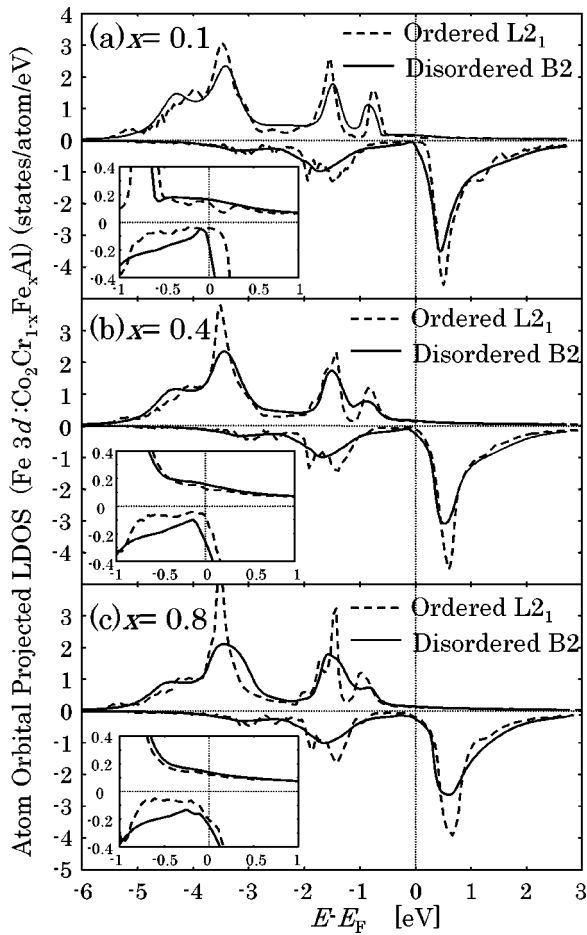


FIG. 6. Atom orbital projected local density of states for the Fe $3d$ of $\text{Co}_2(\text{Cr}_{1-x}\text{Fe}_x)\text{Al}$ with the ordered $L2_1$ structure (solid line) and with the disordered $B2$ structure (broken line): (a) for $x=0.1$; (b) for $x=0.4$; and (c) for $x=0.8$. Each inset shows the magnification of the atom orbital projected local DOS near the Fermi level.

state) as a function of the Fe concentration x in $\text{Co}_2(\text{Cr}_{1-x}\text{Fe}_x)\text{Al}$ with the ordered $L2_1$ structure and the disordered $B2$ structure. Overall we see that the magnetic energy gain increases with increasing x in both the ordered $L2_1$ and the disordered $B2$ structures. This is consistent with the observation that Curie temperature T_C of $\text{Co}_2(\text{Cr}_{0.6}\text{Fe}_{0.4})\text{Al}$ (≈ 600 K) is higher than that of Co_2CrAl (≈ 300 K).²⁶ Furthermore, the magnetic energy gain of the ordered $L2_1$ structure is always larger than that of the disordered $B2$ structure by 0.1 eV. This suggests that $\text{Co}_2(\text{Cr}_{1-x}\text{Fe}_x)\text{Al}$ with the ordered $L2_1$ structure has higher T_C than $\text{Co}_2(\text{Cr}_{1-x}\text{Fe}_x)\text{Al}$ with the disordered $B2$ structure does. Then, we show in Fig. 8 the total energy difference between the ordered $L2_1$ structure and the disordered $B2$ structure of $\text{Co}_2(\text{Cr}_{1-x}\text{Fe}_x)\text{Al}$. In the ferromagnetic state, the ordered $L2_1$ structure is more stable than the disordered $B2$ structure throughout the entire range of x . On the other hand, in the nonmagnetic state, the disordered $B2$ structure is more favorable than the ordered $L2_1$ structure at low Fe concentrations. These results indicate that $\text{Co}_2(\text{Cr}_{1-x}\text{Fe}_x)\text{Al}$ ($x \leq 0.6$) with the ordered $L2_1$ structure is stabilized by the magnetic energy rather than the electrostatic energy. Our results suggest that the fabrication of

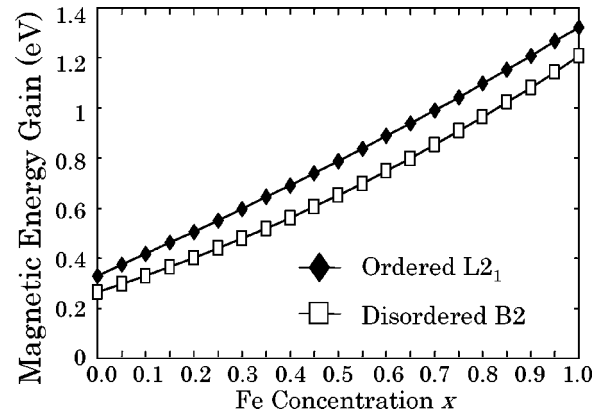


FIG. 7. Magnetic energy gain (energy difference between the ferromagnetic state and the nonmagnetic state) as a function of the Fe concentration x in $\text{Co}_2(\text{Cr}_{1-x}\text{Fe}_x)\text{Al}$ with the ordered $L2_1$ structure (diamond) and the disordered $B2$ structure (square).

$\text{Co}_2(\text{Cr}_{1-x}\text{Fe}_x)\text{Al}$ films with the ordered $L2_1$ structure will be possible if the film is carefully fabricated by, for example, appropriate annealing processes.

The calculated total magnetic moment of $\text{Co}_2(\text{Cr}_{0.6}\text{Fe}_{0.4})\text{Al}$ is $3.88\mu_B$ per unit cell. On the other hand, the observed magnetic moment of thin film $\text{Co}_2(\text{Cr}_{0.6}\text{Fe}_{0.4})\text{Al}$ at 5 K is $2.04\mu_B$ per unit cell.²⁶ The origin of the disagreement between the theoretical and the experimental values of the magnetic moment in $\text{Co}_2(\text{Cr}_{0.6}\text{Fe}_{0.4})\text{Al}$ is unclear at the present stage. However, larger magnetic moments have been obtained for bulk $\text{Co}_2(\text{Cr}_{0.6}\text{Fe}_{0.4})\text{Al}$.^{12,13,25} Furthermore the MCD measurements of core-level absorption for $\text{Co}_2(\text{Cr}_{0.6}\text{Fe}_{0.4})\text{Al}$ by Elmers *et al.*²⁵ showed that the missing magnetic moment compared with the theoretical estimation is mainly due to a reduction of the Cr moment. They suggested that in the experiment the origin of the prominent decrease of the total magnetic moment might be a remaining disorder between Cr and Co. Our calculational results show that the antisite Cr antiferromagnetically couples with the nearest-neighbor ordinary-site Cr, and the total magnetic moment decreases with increasing the disorder level y [see Fig.

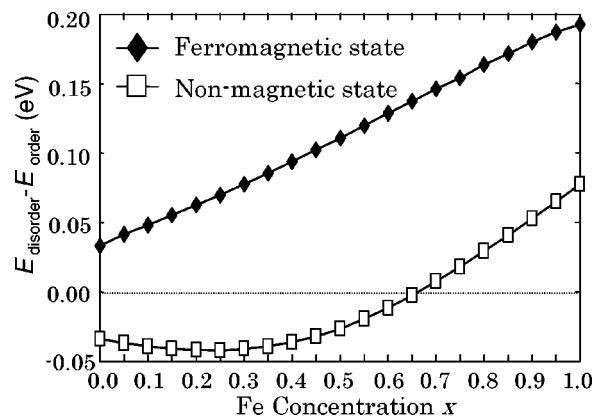


FIG. 8. The total energy difference per unit cell between the ordered $L2_1$ structure and the disordered $B2$ structure of $\text{Co}_2(\text{Cr}_{1-x}\text{Fe}_x)\text{Al}$ as a function of the Fe concentration x for the ferromagnetic state (diamond) and the nonmagnetic state (square).

1(c)]. It is also considered that noncollinear magnetism reduces the magnetic moment of $\text{Co}_2(\text{Cr}_{1-x}\text{Fe}_x)\text{Al}$.³⁸ The possible origins which cause the noncollinear magnetism are (1) the frustration among the local spin moments (if the Cr-Cr coupling is antiferromagnetic, Cr moments at the tetrahedral site are frustrated) and (2) the lowering of local symmetry due to the atomic disorder.³⁹ The former origin can be ignored in $\text{Co}_2(\text{Cr}_{1-x}\text{Fe}_x)\text{Al}$, because relatively large Co moments ($0.75\mu_B$) (Refs. 15–17) align the Cr moments through the ferromagnetic exchange coupling. The latter origin is not significant, because the noncollinear spin configuration caused by the atomic disorder is mainly originated from the spin-orbit coupling,³⁹ which is very small for $3d$ transition-metal elements. Therefore, we consider that the noncollinear magnetism would be irrelevant to the decrease of the magnetic moment of $\text{Co}_2(\text{Cr}_{1-x}\text{Fe}_x)\text{Al}$. Other possibilities, such as nonstoichiometry at surface and interface may also be important in the present system. In the future work, it is very interesting to investigate these points both experimentally and theoretically.

IV. SUMMARY

In this work, we have investigated the effects of atomic disorder on the half-metallicity of the full-Heusler alloy $\text{Co}_2(\text{Cr}_{1-x}\text{Fe}_x)\text{Al}$ on the basis of the first-principles calculation. Our results show that the Cr-Al type disorder does not significantly degrade the half-metallicity of Co_2CrAl , while

the Co-Cr type disorder makes a considerable reduction of the spin polarization. However, the half-metallicity of Co_2CrAl is not practically influenced by the atomic disorder because the total energy of the Co-Cr type disorder is one order of magnitude larger than that of the Cr-Al type disorder. Furthermore, we have found that the substitution of Fe for Cr reduces the spin polarization though it stabilizes the ferromagnetic state of the alloy. It is noted that at low Fe concentrations, the disorder-induced reductions of the spin polarization is prominent while the reductions are not so large, less than about 0.05, in the limiting cases of $x=0.0$ (Co_2CrAl) and $x=1.0$ (Co_2FeAl). We conclude that a highly spin polarized ferromagnet with high T_C will be obtained if a $\text{Co}_2(\text{Cr}_{1-x}\text{Fe}_x)\text{Al}$ with the $L2_1$ structure can be fabricated at low Fe concentrations.

ACKNOWLEDGMENTS

We are grateful to Professor K. Inomata for useful discussions and showing us the experimental data prior to publication. This work was supported in part by a Grant-in-Aid for Scientific Research in Priority Areas “Semiconductor Nanospintronics” (Grants No. 14076105 and No. 14076214) and the IT-program of Research Revolution 2002 (RR2002) “Development of Universal Low-power Spin Memory” from the Ministry of Education, Culture, Sports, Science and Technology (MEXT). Y. M. gratefully acknowledges support from the Murata Science Foundation.

-
- ¹G.A. Prinz, *Science* **282**, 1660 (1998).
²Y. Ohno, D.K. Young, B. Beschoten, F. Matsukura, H. Ohno, and D. Awschalom, *Nature (London)* **402**, 790 (1999).
³S.A. Wolf, D.D. Awschalom, R.A. Buhrman, J.M. Daughton, S. von Molnar, M.L. Roukes, A.Y. Chtchelkanova, and D.M. Treger, *Science* **294**, 1488 (2001).
⁴G. Schmidt, D. Ferrand, L.W. Molenkamp, A.T. Filip, and B.J. van Wees, *Phys. Rev. B* **62**, R4790 (2000).
⁵R.A. de Groot, F.M. Mueller, P.G. van Engen, and K.H.J. Buschow, *Phys. Rev. Lett.* **50**, 2024 (1983).
⁶K. Schwarz, *J. Phys. F: Met. Phys.* **16**, L211 (1986).
⁷W.E. Pickett and D.J. Singh, *Phys. Rev. B* **53**, 1146 (1996).
⁸S. Fujii, S. Ishida, and S. Asano, *J. Phys. Soc. Jpn.* **64**, 185 (1995).
⁹S. Ishida, S. Fujii, S. Kashiwagi, and S. Asano, *J. Phys. Soc. Jpn.* **64**, 2152 (1995).
¹⁰S. Picozzi, A. Continenza, and A.J. Freeman, *Phys. Rev. B* **66**, 094421 (2002); *IEEE Trans. Magn.* **38**, 2895 (2002).
¹¹I. Galanakis, P.H. Dederichs, and N. Papanikolaou, *Phys. Rev. B* **66**, 174429 (2002).
¹²T. Block, Ph.D. thesis, Johannes Gutenberg University Mainz, 2002.
¹³T. Block, C. Felser, G. Jakob, J. Enslin, B. Muhling, P. Gutlich, V. Beaumont, F. Studer, and R.J. Cava, *J. Solid State Chem.* **176**, 646 (2003).
¹⁴I. Galanakis, P.H. Dederichs, and N. Papanikolaou, *Phys. Rev. B* **66**, 134428 (2002).
¹⁵M. Shirai, T. Ogawa, I. Kitagawa, and N. Suzuki, *J. Magn. Magn. Mater.* **177-181**, 1383 (1998).
¹⁶H. Akinaga, T. Manago, and M. Shirai, *Jpn. J. Appl. Phys., Part 2* **39**, L1118 (2000).
¹⁷M. Shirai, *Physica E (Amsterdam)* **10**, 143 (2001); M. Shirai, *J. Appl. Phys.* **93**, 6844 (2003).
¹⁸P.R. Broussard, S.B. Qadri, V.M. Browning, and V.C. Cestone, *Appl. Surf. Sci.* **115**, 80 (1997).
¹⁹R.J. Soulen, Jr., J.M. Byers, M.S. Osofsky, B. Nadgorny, T. Ambrose, S.F. Cheng, P.R. Broussard, C.T. Tanaka, J. Nowak, J.S. Moodera, A. Barry, and J.M.D. Coey, *Science* **282**, 85 (1998).
²⁰J.A. Caballero, A.C. Reilly, Y. Hao, J. Bass, W.P. Pratt, Jr., F. Petroff, and J.R. Childress, *J. Magn. Magn. Mater.* **198-199**, 55 (1999).
²¹T. Ambrose, J.J. Krebs, and G.A. Prinz, *Appl. Phys. Lett.* **76**, 3280 (2000).
²²M.P. Raphael, B. Ravel, M.A. Willard, S.F. Cheng, B.N. Das, R.M. Stroud, K.M. Bussmann, J.H. Claassen, and V.G. Harris, *Appl. Phys. Lett.* **79**, 4396 (2001).
²³B. Ravel, M.P. Raphael, V.G. Harris, and Q. Huang, *Phys. Rev. B* **65**, 184431 (2002).
²⁴U. Geiersbach, A. Bergmann, and K. Westerholt, *J. Magn. Magn. Mater.* **240**, 546 (2002).
²⁵H.J. Elmers, G.H. Fecher, D. Valdaitsev, S.A. Nepijko, A. Gloskovskii, G. Jakob, G. Schönhense, S. Wurmehl, T. Block, C. Felser, P.-C. Hsu, W.-L. Tsai, and S. Cramm, *Phys. Rev. B* **67**, 104412 (2003).

- ²⁶K. Inomata, S. Okamura, R. Goto, and N. Tezuka, *Jpn. J. Appl. Phys.* **42**, L419 (2003).
- ²⁷D. Orgassa, H. Fujiwara, T.C. Schulthess, and W.H. Butler, *Phys. Rev. B* **60**, 13 237 (1999).
- ²⁸D. Orgassa, H. Fujiwara, T.C. Schulthess, and W.H. Butler, *J. Appl. Phys.* **87**, 5870 (2000).
- ²⁹I. Galanakis, *J. Phys.: Condens. Matter* (to be published).
- ³⁰I. Galanakis, *J. Phys.: Condens. Matter* **14**, 6329 (2002).
- ³¹W. Kohn and N. Rostoker, *Phys. Rev.* **94**, 1111 (1954).
- ³²H. Akai and P.H. Dederichs, *Phys. Rev. B* **47**, 8739 (1993).
- ³³M. Rasolt and D.J.W. Geldart, *Phys. Rev. B* **34**, 1325 (1986).
- ³⁴K.R.A. Ziebeck and P.J. Webster, *J. Phys. Chem. Solids* **35**, 1 (1974).
- ³⁵P.J. Webster, *J. Phys. Chem. Solids* **32**, 1221 (1971).
- ³⁶K.H.J. Buschow and P.G. van Engen, *J. Magn. Magn. Mater.* **25**, 90 (1981).
- ³⁷W. Kohn and L.J. Sham, *Phys. Rev.* **140**, 1133 (1965).
- ³⁸J. Enkovaara, A. Ayuela, J. Jalkanen, L. Nordström, and R.M. Nieminen, *Phys. Rev. B* **67**, 054417 (2003).
- ³⁹*Electronic Structure and Magnetism of Complex Systems* (Springer, Berlin, 2003), p. 224.